BIOCHEMISTRY
including biophysical chemistry & molecular biology
Article

Biochemistry **2009,** *48,* 11929–11938 11929
DOI: 10.1021/bi901775j

Dss1 Regulates Interaction of Brh2 with DNA†

Qingwen Zhou, Nayef Mazloum, Ninghui Mao, Milorad Kojic, and William K. Holloman*

Department of Microbiology and Immunology, Weill Cornell Medical College, New York, New York 10065

Received May 10, 2009; Revised Manuscript Received November 16, 2009

ABSTRACT: Brh2, the BRCA2 homologue in *Ustilago maydis*, plays a crucial role in homologous recombination by controlling Rad51. In turn, Brh2 is governed by Dss1, an intrinsically disordered protein that forms a tight complex with the C-terminal region of Brh2. This region of the protein associating with Dss1 is highly conserved in sequence and by comparison with mammalian BRCA2 corresponds to a part of the DNA binding domain with characteristic OB folds. The N-terminal region of Brh2 harbors a less-defined but powerful DNA binding site, the activity of which is revealed upon deletion of the C-terminal region. Full-length Brh2 complexed with Dss1 binds DNA slowly, while the N-terminal fragment binds quickly. The DNA binding activity of full-length Brh2 appears to correlate with dissociation of Dss1. Addition of Dss1 to the heterotypic Brh2−Dss1 complex attenuates DNA binding activity, but not by direct competition for the N-terminal DNA binding site. Conversely, the Brh2−Dss1 complex dissociates more quickly when DNA is present. These findings suggest a model in which binding of Brh2 to DNA is subject to allosteric regulation by Dss1.

In eukaryotes, Rad51 is essential for repair of DNA damage by homologous recombination (*1*). Rad51 assembles into a complex with single-stranded (ss)[1] DNA that has been exposed after some processing of the damaged duplex to form a nucleoprotein filament, which is the catalytically active form of Rad51 for promoting homologous pairing and DNA strand exchange. BRCA2 is an important regulator of Rad51 activity (*2*, *3*) and appears to exert both positive and negative effects on Rad51 filaments (*4*−*7*). Biochemical studies with Brh2, the BRCA2 homologue from the fungus *Ustilago maydis*, have demonstrated that it mediates Rad51 assembly on a protruding 3′-single-strand DNA tail (*8*) and interacts with Rad51 in other ways to promote poststrand invasion steps in recombination (*9*). Interaction of Rad51 with Brh2 occurs through the single BRC element located in the N-terminal region of the protein (*10*) and a second and less well-defined domain, the CRE, located at the extreme C-terminus (*11*). These N-terminal and C-terminal domains participate with each other in some as yet unknown way to direct proper Rad51 filament assembly. The process depends on Dss1 (*11*), a small versatile acidic protein that physically interacts with Brh2 through a region corresponding to the DSS1/DNA binding domain (DBD) in mammalian BRCA2 (*12*). The mammalian BRCA2 DBD consists of a tandem array of three OB (oligonucleotide/oligosaccharide binding) folds and a helix-rich domain that is laced to the adjacent OB fold by intertwining with DSS1 (*13*). Sequence alignment with BRCA2 indicates that a region corresponding to part of the helix-rich domain and the adjacent OB1 and OB2 folds is conserved in Brh2, but that OB3 is absent. In Brh2, 36 of the 40 residues in the BRCA2 DBD that contact DSS1 are identical or conserved (*12*).

The single amino acid change W728A in *U. maydis* Brh2 abolishes its capacity to bind Dss1 and support DNA repair (*11*). In the same vein, deletion of the gene encoding Dss1 in *U. maydis* causes extreme sensitivity to DNA damage and deficiency in recombination, effectively phenocopying the *brh2* mutant (*12*, *14*). In view of the physical interaction between Brh2 and Dss1, these genetic findings are consistent with the idea that Dss1 serves as a needed cofactor or as a direct activator of Brh2. Other studies, however, support the view that Dss1 interacts with Brh2 in a more complex way to counteract autoinhibition. Removal of a tract of 40 amino acids from the C-terminus of Brh2 is enough to cause complete loss of activity in complementing the UV sensitivity of the *brh2* mutant, yet paradoxically, via removal of a much longer tract from the C-terminus that encompasses the entire Dss1/DNA binding domain (the DBD), radiation resistance can be substantially restored not only in the *brh2* mutant but also in the *dss1* mutant (*15*). Furthermore, expression of the N-terminal fragment in the *brh2* mutant restores Rad51 focus formation and allelic recombination proficiency to an even higher level than in wild-type cells (*15*). These results imply that the DBD deletion removes a negative regulatory function from Brh2 that is countermanded by Dss1.

Functional complementation of the *brh2* and *dss1* mutants by the Brh2 N-terminal fragment ($Brh2^{1-551}$ or $Brh2^{NT}$) with the DBD deleted strongly suggests that this truncated protein has an inherent ability to organize Rad51, mediate delivery of Rad51 to sites of DNA damage, and support DNA repair in a manner independent of Dss1 modulation. To account for all of these functions, we supposed that the N-terminal region would contain an intrinsic DNA binding capacity, and indeed as predicted, we found it has the capacity to bind DNA with an affinity and specificity for structure reflecting the properties of the full-length

†This work was supported in part by Grants GM42482 and GM79859 from the National Institutes of Health.

*To whom correspondence should be addressed. Telephone: (212) 746-6510. Fax: (212) 746-8587. E-mail: wkhollo@med.cornell.edu.

[1]Abbreviations: BRC, Rad51 binding element; CRE, C-terminal Rad51 binding element; CT, carboxy-terminal; DBD, DSS1/DNA binding domain; ds, double-stranded; HEPES, *N*-(2-hydroxyethyl)piperazine-*N*′-2-ethanesulfonic acid; His tag, hexahistidine tag; MBP, maltose binding protein; NT, amino-terminal; NTA, nitrilotriacetate agarose; OB, oligonucleotide/oligosaccharide binding; oligo dT, oligothymidylate; ss, single-stranded; UV, ultraviolet.

Published on Web 11/17/2009

protein (*16*). By comparison, the C-terminal region (Brh2$^{505-1075}$ or Brh2^{CT}) corresponding to the canonical DBD bound DNA less tightly by 1 order of magnitude, as did the DBD of mouse BRCA2. These results imply that the primary interaction site in Brh2 for association with DNA resides in the N-terminal fragment.

Taken altogether, the model for Brh2 that emerges suggests an architectural arrangement featuring an N-terminal DNA binding domain coupled to a C-terminal regulatory domain that responds to Dss1. What is not clear is how these functional modules communicate. If Dss1 is required for appropriately controlled functional activity in the context of the full-length Brh2 protein, then it follows that Dss1 imposes order and/or governs cooperation between the two protein domains. Thus, the hypothesis framed by these observations is that Dss1 exerts control over DNA binding through the N-terminal domain even though the only known site for physical interaction of Dss1 with Brh2 is limited to the C-terminal domain. Here we have investigated the relationship between binding of DNA to Brh2 and association with Dss1.

EXPERIMENTAL PROCEDURES

U. maydis Methodology. Manipulations of *U. maydis* strains, culture methods, gene transfer procedures, and survival after UV irradiation have been described previously (*17*). *U. maydis* strains included UCM350 (nominal wild type) and UCM591 (Δ*dss1*). Dss1 and the mutant derivative Dss1^{D37A} were expressed from autonomously replicating plasmids with the *gap* (glyceraldehyde-3-phosphate dehydrogenase) promoter driving expression and with hygromycin resistance as the selectable marker. Dss1^{D37A} was constructed using overlapping oligonucleotides and a PCR methodology (*18*). For spot assays for cell survival, cell suspensions of overnight cultures were adjusted to $\sim 2 \times 10^7$ cells per mL, diluted in 10-fold serial dilutions, and aliquots (10 μL) of each were spotted on agar medium. Survival is indicated as growth of colonies 3 days after irradiation.

Protein Preparations. Brh2 and Brh2^{CT} proteins tagged with MBP in complex with His-tagged Dss1 were purified after overexpression in *Escherichia coli* as described previously (*11*, *19*). Briefly, purification involved sequential affinity chromatography steps on Ni^{2+}-NTA (nitrilotriacetic acid agarose, Qiagen) and cross-linked amylose resin (New England Biolabs), in which the protein was eluted specifically with imidazole and maltose, respectively, followed by salt gradient elution off a column of monoQ beads using an AKTA FPLC system (GE Healthcare). Brh2^{CT} protein devoid of MBP tag was prepared from a fusion protein which was engineered to contain a tobacco etch virus (TEV) protease recognition site in the linker regions connecting the MBP tag to Brh2^{CT} as described previously (*16*). After cleavage with TEV protease, Brh2^{CT} was purified by salt gradient elution from monoQ resin. Brh2^{NT} terminating at residue M551 was purified as a fusion protein with an N-terminal MBP tag and C-terminal His tag. Purification followed the same protocol developed for the full-length protein but included an additional step of salt gradient elution from HiTrap heparin-agarose (GE Healthcare). The Brh2−Dss1 complex used in preparation of the Brh2 apoprotein free of Dss1 was purified as described above except that it was eluted from amylose resin using 1.0 M α-methyl glucoside instead of 10 mM maltose to facilitate rebinding of Brh2 to amylose resin in a subsequent step . After elution of the Brh2−Dss1 complex from the monoQ column, the fraction was brought to 20 mM $MgCl_2$, held at 37 °C for 1 h, and then loaded on a column of cross-linked amylose at 4 °C. The column was washed with 50 volumes of buffer A [25 mM Tris-HCl (pH 7.5), 200 mM KCl, 1 mM DTT, 1 mM EDTA, and 10% glycerol] containing 20 mM $MgCl_2$ to remove Dss1, and then Brh2 was eluted with buffer A containing 10 mM maltose. Proteins were stored in buffer A. His-tagged Dss1 and Dss1^{D37A} were purified after expression in *E. coli*. The procedure included affinity purification on Ni^{2+}-NTA, gradient elution from monoQ beads, and molecular sieve chromatography on a Superose 6 gel filtration column. A form of His-tagged Dss1 (His-PK-Dss1) containing a target sequence that could be phosphorylated and thus labeled with ^{32}P using [γ-^{32}P]ATP and human protein kinase A (PKA) catalytic subunit (Sigma-Aldrich) was engineered via insertion of an oligonucleotide encoding the PKA amino acid recognition sequence (LRRASV) into the His-Dss1 gene fusion between the hexahistidine coding sequence and Dss1 open reading frame. When MBP-Brh2 and His-PK-Dss1 were coexpressed and purified as a heterotypic complex as above, His-PK-Dss1 could be specifically labeled in situ with ^{32}P using the PKA catalytic subunit. There was no detectable labeling of the associated MBP-Brh2 protein. Phosphorylation was performed in reaction mixtures containing 25 mM Tris-HCl (pH 7.5), 50 mM KCl, 5 mM $MgCl_2$, 12.5 nM [γ-^{32}P]ATP, 500 nM MBP-Brh2−His-PK-Dss1 protein, and 5 units/mL PKA catalytic subunit for 16 h at 4 °C. ^{32}P-labeled MBP-Brh2−His-PK-Dss1 protein was obtained after purification through Ni^{2+}-NTA beads and amylose resin as described above, eluted from the latter with α-methyl glucoside.

DNA Binding. DNA binding was assayed by three methods. Electrophoretic mobility shift assays were performed using a single-stranded 60mer oligonucleotide (ss60mer) GCTGCGCAAGGATAGGTCGAATTTTCTCATTTTCCGCCAGCAGTCCACTTCGATTTAATT (derived from phage ϕX174 sequence) labeled at the 5′-end with ^{32}P using polynucleotide kinase and [γ-^{32}P]ATP or else the fluorescent dye IRD700 or IRD800 (MWG Biotech AG) as the substrate (*16*). Binding reaction mixtures contained 3.3 nM ss60mer and protein as required in reaction buffer [25 mM HEPES (pH 7.5), 60 mM KCl, and 2 mM $MgCl_2$]. After incubation at 37 °C, glutaraldehyde was added to a final concentration of 0.2%. Fixation was continued for 10 min and quenched with 100 mM Tris-HCl (pH 8.0). Products were monitored after electrophoresis at room temperature in 1% agarose gels cast in 40 mM Tris-acetate (pH 7.6). Gel images were collected with an Odyssey infrared detection platform (LI-COR Biosciences) or with a phosphorimager and quantified with ImageQuaNT (Molecular Dynamics). Nitrocellulose filter binding assays were performed using 5′-^{32}P-labeled ss60mer as described above, but reactions were processed by washing solutions through a double layer of nitrocellulose membrane (Bio-Rad Laboratories) and DEAE-celluose paper (Whatman DE81) in a dot-blot manifold (*20*). Radiographic images were collected with a phosphorimager and quantified. Fluorescence polarization assays were performed in reactions (100 μL) using 5′-fluorescein-labeled ss49mer (MWG Biotech AG) that was derived from plasmid pBluescript II SK+ (Stratagene) and described previously as 49mer(+) (*19*). Measurements were taken at room temperature using a SpectraMax M5 multilabel plate reader (Molecular Devices) 30 min after samples had been mixed in white, flat-bottomed 96-well assay plates (Corning). Excitation was set at 492 nm and emission at 525 nm with a 515 nm cutoff filter. The *G* factor was set at

1.0. Anisotropy was determined using internal software of the instrument. All DNA concentrations are expressed in moles of molecules, rather than nucleotide, unless explicitly stated.

Pull-Down Procedures. Brh2 or Brh2^{CT} complexed with His-Dss1 was added to mixes (60 μL) containing reaction buffer and DNA (ss60mer as described above) as required to a final concentration of 550 nM and held at 37 °C. At specified times, the mixes were transferred to a tube containing 30 μL of a settled slurry of affinity beads (Ni^{2+}-NTA or amylose resin as appropriate) and held on ice for 10 min. After brief centrifugation, the beads were collected and protein in the supernatant and bound fractions was analyzed by electrophoresis in polyacrylamide gels containing SDS. Protein was visualized by staining with SimplyBlue SafeStain (Invitrogen). When necessary to visualize the DNA, the IRD800 ss60mer with the identical sequence was added at a molar ratio of 1:50 with respect to unlabeled DNA. DNA was detected with the Odyssey infrared detection platform (LI-COR Biosciences). As an alternative method, Brh2 complexed with ^{32}P-labeled His-PK-Dss1 was added to reaction mixes containing 3′-biotin-labeled ss60mer (phage ϕX174 sequence as described above, from MWG Biotech AG). The 3′-biotin-labeled ss60mer annealed with partially complementary 5′-IRD700-labeled 80mer (CGAATTAAATCGAAGTGGACTGCTGGCGGAAAATGAGAAAATTCGACCTATCCTTGCGCAGCTCGAGAAGCTCTTACTTT) was added as a spike (1:50 molar ratio with respect to ss60mer) to reaction mixes to enable visualization of the DNA. After incubation, mixes (15 μL) were transferred to a tube containing 10 μg of streptavidin-coated magnetic particles (Pierce), which were collected with a magnet, and the unbound fraction was set aside. The beads were washed with two (100 μL) rinses of reaction buffer. Protein (and DNA) in the bound and unbound fractions was analyzed by SDS−gel electrophoresis and visualized by staining, phosphorimaging, and infrared dye detection.

Reconstitution of the Brh2−Dss1 Complex. Brh2 apoprotein (30 nM) free of Dss1 was added to mixes (0.5 mL) containing 25 mM Tris-HCl (pH 7.5), 25 mM KCl, 4 mM $MgCl_2$, 1 mM DTT, and 10% glycerol with 250 nM His-Dss1. After 1 h at 4 °C, 100 μL of packed Ni^{2+}-NTA beaded resin was added and the slurry mixed for 10 min. Beads were collected by centrifugation and washed twice (0.5 mL each) with 25 mM Tris-HCl (pH 7.5), 200 mM KCl, 20 mM imidazole, 0.1% NP-40, 10% glycerol, and protein in the supernatant, and bound fractions were analyzed by electrophoresis in polyacrylamide gels containing SDS.

RESULTS

Complexes Formed by Addition of the Brh2−Dss1 Complex or Brh2^{NT} to DNA. In the experiments described below, we used Brh2^{NT} (Brh2$^{1-551}$), full-length Brh2 (Brh2$^{1-1075}$), and Brh2^{CT} (Brh2$^{505-1075}$), the latter two necessarily being produced as heterotypic complexes with Dss1 (His-tagged). We have referred to these latter complexes in the past as Brh2 and Brh2^{CT}, respectively, for the sake of simplicity, but to avoid confusion in this work, we will indicate Brh2−Dss1 or Brh2^{CT}−Dss1 when the heterotypic complex was used in reactions. Purification of these proteins as well as Dss1 and their analyses by SDS gel electrophoresis have been described and documented in previous work (*11*, *16*, *19*). We also demonstrated in those previous studies that the affinity tags did not interfere with the biological activity of the proteins as measured by complementation activity.

This work evolved from studies on the DNA structure preference exhibited by Brh2−Dss1 and Brh2^{NT} in binding reactions using the electrophoretic mobility shift assay (*16*, *19*). Experimentation was performed at protein concentrations sufficiently low that the DNA binding activity observed was due predominantly to the primary interaction site located in the N-terminal region of Brh2 (*16*). As the substrate, we used a single-stranded mixed sequence oligonucleotide of 60 nucleotides labeled at the 5′-end with ^{32}P or the IRD fluorophore (*16*). A mixed sequence oligonucleotide was used as a substrate rather than oligo dT, because the latter bound so poorly that complexes were minimally detectable at the protein concentrations used (data not shown). A length of 60 residues was chosen because it was a good substrate in D-loop reactions performed in related studies with Rad51, and it was above an apparent minimum of ~30 residues necessary for efficient formation of the complex with Brh2 (data not shown). Under our reaction conditions, protein−DNA complexes were unstable. Therefore, we incorporated a glutaraldehyde fixation step so that complexes could be visualized with more clarity (Figure 1A). Here as in previous studies (*16*) we found that Brh2−Dss1 and Brh2^{NT} bound natural mixed sequence ss60mer or ss100mer with approximately the same avidity and formed discrete complexes. Low concentrations of Brh2−Dss1 complexes ran with faster mobility than the Brh2^{NT}−DNA complexes, in spite of the greater mass (in Figure 1B, compare lanes d−g). With increasing concentrations of Brh2−Dss1, DNA complexes with slower mobility formed, while with increasing concentrations of Brh2^{NT}, the complexes ran more uniformly, and even with slightly faster mobilities at higher concentrations. As the mobility shift assay was performed after addition of glutaraldehyde, it is possible that the fixation contributed to anomalies in the mobilities of the complexes. It is also possible that the protein−DNA complexes changed in conformation as a function of concentration, that protein−protein interactions contributed to the differences in mobilities, or that the DNA secondary structure of the mixed sequence oligonucleotides was contributory.

As an alternative means of determination, we assessed DNA binding by the classic nitrocellulose filter retention method (*20*), which does not rely on a fixation step but simply traps protein−DNA complexes on a porous membrane of nitrocellulose pretreated to weaken binding of free single-stranded DNA (Figure 1C). A second layer of DEAE paper captures the free DNA. An advantage of this assay is that binding reactions can be stopped in seconds simply by passing reaction mixes through the filter to remove uncomplexed components and so can be used to monitor rates of binding. Nevertheless, the method does not give a true measure of equilibrium, can be inefficient at trapping complexes, and does not necessarily yield any additional information about the nature of protein−DNA complexes formed. When performed side by side, the nitrocellulose filter assay was less cumbersome than the mobility shift assay but was less sensitive at detecting complexes formed at lower concentrations of Brh2−Dss1 and Brh2^{NT} (Figure 1D) and unfortunately gave us no further insight into the basis for the mobility differences noted above.

Finally, we used fluorescence polarization as a means of verifying binding. An advantage of this method is that observations are made in real time and require no perturbation of the system. A change in anisotropy was evident upon addition of Brh2−Dss1 or Brh2^{NT} to a fluorescein-labeled ss49mer. The magnitudes of change were virtually identical, and the binding

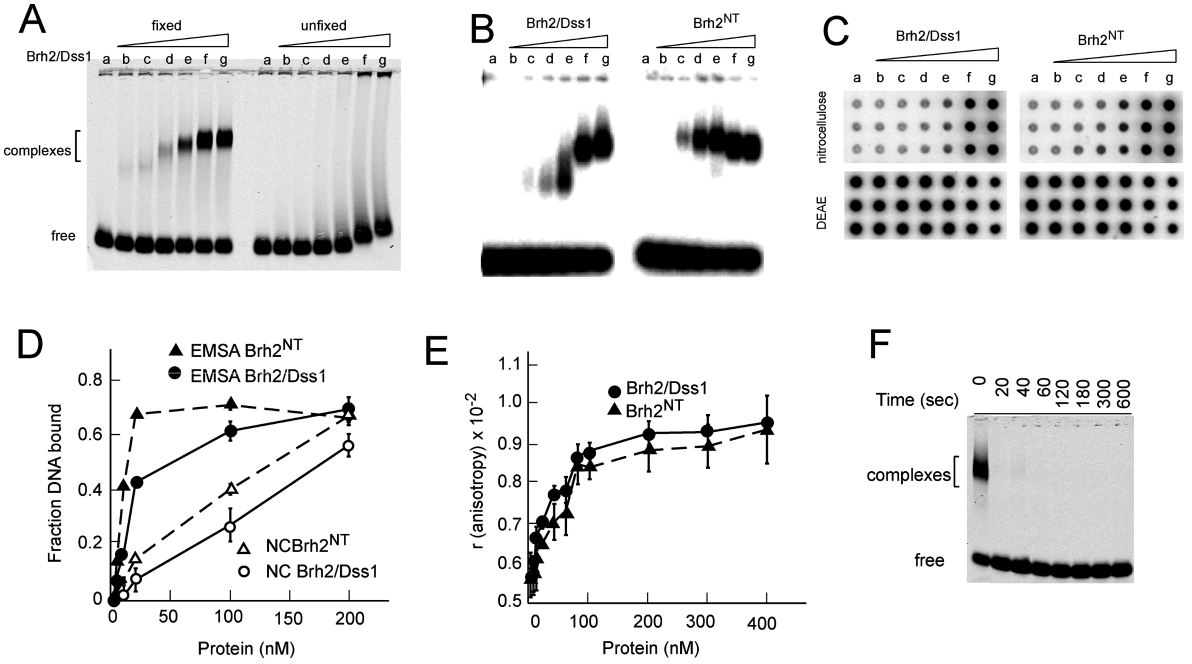

FIGURE 1: DNA binding assays. (A) Binding reaction mixtures containing IRD800 ss60mer and Brh2−Dss1 at the concentrations indicated were incubated for 40 min. Samples were either fixed with glutaraldehyde before electrophoresis or run without fixation: lane a, no protein; lane b, 2 nM protein; lane c, 4 nM protein; lane d, 10 nM protein; lane e, 20 nM protein; lane f, 100 nM protein; and lane g, 200 nM protein. (B) ^{32}P-labeled ss100mer was incubated with Brh2−Dss1 or Brh2^{NT} at the concentrations indicated in panel A, and samples were fixed with glutaraldehyde. (C) Reaction mixes with ^{32}P-labeled ss60mer incubated with Brh2−Dss1 or Brh2^{NT} at the concentrations indicated in panel A were passed onto a manifold through a double-layer sandwich of nitrocellulose and DEAE-cellulose membrane. (D) Quantification of the results in panels B and C. (E) Binding reaction mixtures containing 5′-fluorescein-labeled 49mer and Brh2−Dss1 at the indicated concentrations were incubated for 20 min, and then the anisotropy was determined. (F) Sample mixes containing 100 nM Brh2−Dss1 but no DNA were set up. Glutaraldehyde was then added to samples, and the samples were incubated for the indicated times before the binding reaction was initiated via addition of IRD800 ss60mer. After further incubation for 20 min, samples were analyzed by gel electrophoresis.

isotherms were essentially superimposable. These findings support the notion that the masses of the complexes formed are comparable in the case of Brh2−Dss1 and Brh2^{NT} and also agree with the results from the mobility shift assay that their binding affinities are approximately the same. The instrument we used was not well-suited for monitoring association rates.

For our purposes, the mobility shift assay was excellent for measuring protein−DNA complexes with Brh2−Dss1 and Brh2^{NT} in terms of sensitivity and in discerning differences in the nature of the protein−DNA complexes formed, although the basis of the differences remains unclear. While not ideal for examining association kinetics, the assay works to our advantage when the glutaraldehyde fixation step is incorporated as the fixative abolishes Brh2 binding activity within a matter of seconds, effectively quenching the reaction (Figure 1F) as well as stabilizing the complexes (Figure 1A). Thus, the assay can suffice for detecting gross differences in binding rates and can be useful in distinguishing qualitative differences in various types of complexes formed. Knowledge of the basis of the differences will require analysis by a more sophisticated methodology such as surface plasmon resonance and is beyond the scope of this study.

Association of Brh2−Dss1 with DNA Is Slow Compared to That of Brh2^{NT}. A striking difference that we noted between full-length Brh2−Dss1 and Brh2^{NT} in the binding reactions was that full-length Brh2−Dss1 bound DNA more slowly than Brh2^{NT} (Figure 2). Formation of protein−DNA complexes with two different concentrations of Brh2^{NT} was fast with a half-time of seconds and approached a plateau level within 1 min. On the other hand, formation of complexes between full-length Brh2−Dss1 and DNA followed apparently hyperbolic association kinetics, but at a slower rate that was dependent on the protein concentration. Similar observations were made using both the mobility shift and nitrocellulose filter binding assays (compare Figure 2B,C with Figure 2E,F). We had assumed that the association of Brh2−Dss1 and derivatives with DNA was diffusion-controlled and would be rapid as is commonly observed with DNA binding proteins. The fast association of Brh2^{NT} with DNA was consistent with our expectations for a diffusion-controlled binding reaction, but the slow formation of protein−DNA complexes with full-length Brh2 was surprising and raised the notion that another process was rate-limiting in the binding reaction.

Dissociation of Brh2−Dss1 Is Enhanced by DNA. A working model would suggest that a change in the state of the protein might be necessary to reveal the strong N-terminal DNA binding domain. As Brh2 was purified as a heterotypic protein complex with Dss1, we suspected that Dss1 would be most likely responsible for regulating any change in the state of Brh2. Therefore, we examined the Brh2−Dss1 complex after addition of DNA. We took advantage of the His tag on Dss1 as a means of selectively separating Brh2 molecules complexed with Dss1 from those free of Dss1 by a pull-down procedure using Ni^{2+}-nitrilotriacetate agarose (Ni^{2+}-NTA) beads (Figure 3, schematic). Ni^{2+}-NTA beads were added to a solution containing the Brh2−Dss1 complex and collected by centrifugation, and the protein in the supernatant and bound fractions was analyzed by SDS gel electrophoresis and detected by staining the gels with SimplyBlue SafeStain. This stain was advantageous in detecting Dss1, which because of its small size and disordered structure (see below) was problematic in detection and would leach out of gels particularly under the prolonged acidic soaking and washing

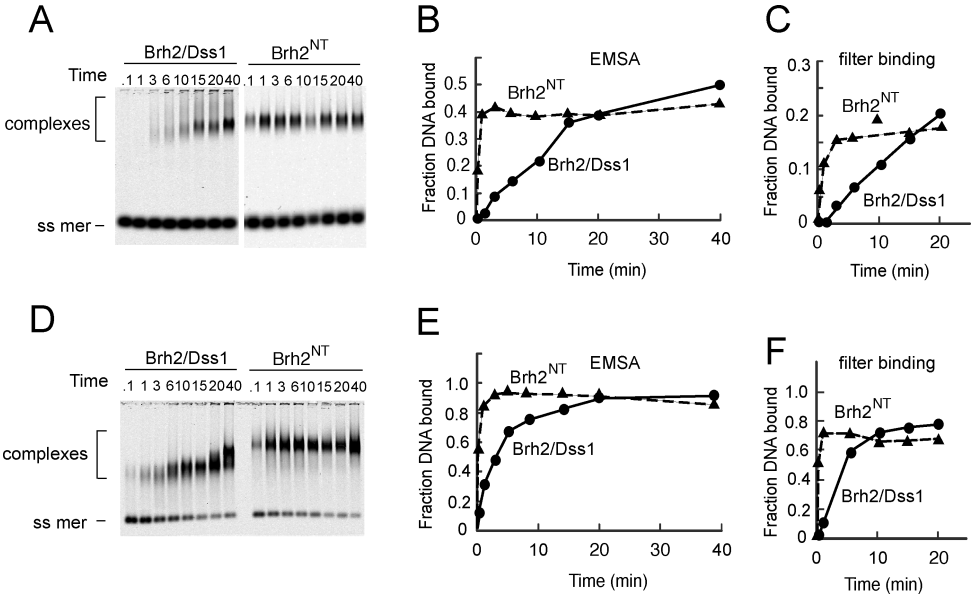

FIGURE 2: DNA binding rates. Time courses of DNA binding were determined with single-stranded oligonucleotide and Brh2 or Brh2^{NT}. Aliquots were removed from binding reaction mixtures at the indicated times and mixed with glutaraldehyde, and the DNA was analyzed for mobility shift after electrophoresis. The fraction of DNA bound was quantified from the relative intensity of the free and shifted oligomer and is shown graphically below: (A) Brh2 or Brh2^{NT} at 20 nM and (B) Brh2 or Brh2^{NT} at 100 nM.

conditions used in staining with Coomassie brilliant blue. With Brh2−Dss1 samples held on ice, there was a small fraction of Brh2 (< 10%) that was not captured by the beads. This baseline level represents Brh2−Dss1 complex that simply escaped capture from the Ni^{2+}-NTA beads and Brh2 molecules in the preparation free of Dss1. After incubation at 37 °C in buffer containing a modest salt concentration, there was only slight dissociation of the Brh2−Dss1 complex which is evident in the marginal increase in the level of Brh2 in the supernatant (Figure 3A). When DNA was added, however, Brh2 became almost quantitatively dissociated from Dss1 (Figure 3A). In this particular experiment (Figure 3A), Dss1 was hardly visible after the staining procedure. With an input of 500 nM Brh2−Dss1 complex, 130 nM ss60mer (~1 ss60mer oligonucleotide per 4 Brh2 molecules) was sufficient to promote maximal dissociation (Figure 3B). Brh2 in the bound fraction was recovered in two forms after elution from the beads which is evident in the SDS gels. One form ran with the mass usually observed (~170 kDa), while the second ran with an apparent mass of at least twice that. This is most likely the result of a Ni^{2+}-mediated oxidative cross-linking reaction that occurred during processing the samples. Such intermolecular cross-linking with His-tagged proteins has been documented (*21*).

Brh2 Bound to DNA Is Free of Dss1. The experiment described above suggested that Dss1 dissociates from Brh2 in the presence of DNA. To investigate this point, we asked about the status of Dss1 once DNA became bound to Brh2. Two approaches were taken using a version of Dss1 labeled with ^{32}P so that it could be tracked more easily. For this purpose, the protein was engineered to contain a target sequence for protein kinase A that enabled ^{32}P radiolabeling. With the further addition of fluorescently labeled ss60mer DNA as a substrate, we were able to track the fate of all three components after mixing. In the first approach, following incubation of the Brh2−Dss1 complex (MBP-Brh2−[^{32}P]His-PK-Dss1) with or without DNA, Ni^{2+}-NTA beads were added to trap Dss1 (Figure 4A). The unbound fraction was collected and was added to amylose resin to trap Brh2. As is evident (Figure 4A) when no DNA was present, the bulk of the Brh2 was retained on the Ni^{2+}-NTA beads together with the Dss1. Brh2 that was not retained by the Ni^{2+}-NTA beads was pulled down with amylose resin and had little associated Dss1. When DNA was present, the amount of Brh2 retained by the Ni^{2+}-NTA beads was substantially reduced and little DNA was trapped. The bulk of the Brh2 and large fraction of the DNA was trapped by amylose beads. There was little Dss1 in this fraction.

In the second approach, the DNA was biotin-labeled ss60mer spiked with a small amount hybridized to a partially complementary fluorescently labeled ss80mer (Figure 4B). After incubation with the Brh2−Dss1 complex, the DNA was trapped on streptavidin-coated beads, and the bound components were analyzed (Figure 4B). The bulk of the Brh2 was present in the DNA-bound fraction, while the bulk of the Dss1 was in the supernatant. Conversely, when no DNA was added, only a background level of Brh2 was associated with the beads. Taken together, these results indicate that Dss1 is no longer associated with Brh2 when it is bound to DNA.

Excess Dss1 Inhibits Binding of the Brh2−Dss1 Complex to DNA. From the crystal structure determination of the murine BRCA2 DBD, it was found that DSS1 bound to a face of the molecule on the opposite side of the OB fold DNA binding groove (*13*). Nevertheless, because Dss1 is a highly acidic polypeptide with interspersed hydrophobic and aromatic residues, it was proposed as a DNA mimic with possible regulatory capability. In view of our localizing the predominant DNA binding domain within Brh2 to the N-terminal region (*16*), we considered the possibility that Dss1 interacted with this domain in Brh2^{NT} as well as with the canonical C-terminal region corresponding to the face of the DBD opposite the OB fold DNA binding channel. If Dss1 bound to the DNA binding domain within the N-terminal region, it would be expected to compete with DNA for binding to Brh2^{NT}. Upon testing this notion, we found that increasing the level of Dss1 had no effect on the ability of Brh2^{NT} to bind DNA. Addition of increasing levels of Dss1 to Brh2−Dss1, however, resulted in a corresponding

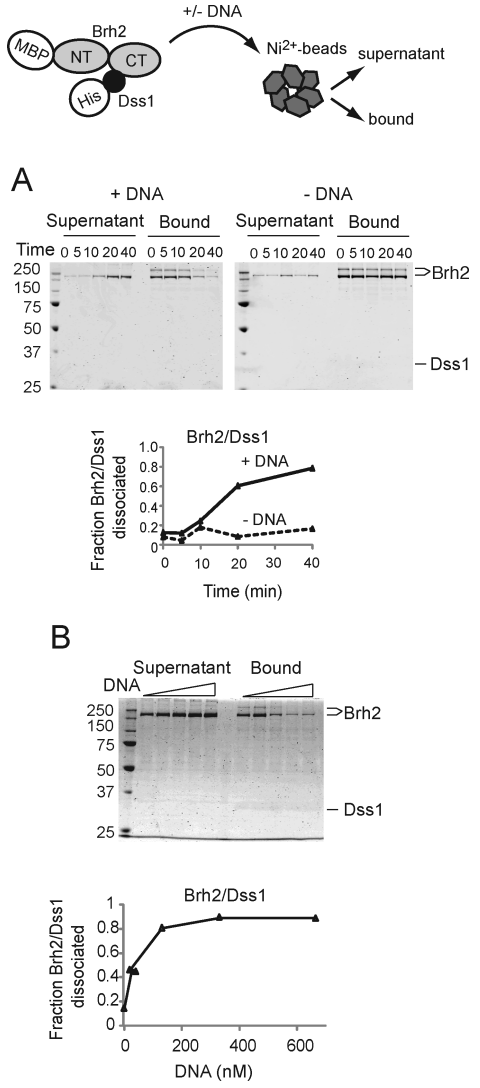

FIGURE 3: Dissociation of Brh2−Dss1 complexes. MBP-tagged Brh2 (represented as N-terminal and C-terminal lobes) complexes with His-tagged Dss1 (black circle) are mixed with Ni^{2+}-NTA beads. (A) The Brh2−His-Dss1 complex (550 nM) was incubated at 37 °C in the presence or absence of DNA (130 nM unlabeled ss60mer). At the indicated times (minutes), Ni^{2+}-NTA beads were added to pull down His-Dss1 either free or complexed with Brh2. The protein composition in the supernatant or bound fractions was determined by SDS gel electrophoresis. Protein was visualized by staining with SimplyBlue SafeStain (Invitrogen). The time course of dissociation is shown graphically. (B) Reaction mixes contained Brh2−His-Dss1 complex (550 nM), and increasing concentrations of DNA (20, 40, 130, 330, and 660 nM from left to right) were incubated for 20 min. The zero point for no DNA added was taken from panel A.

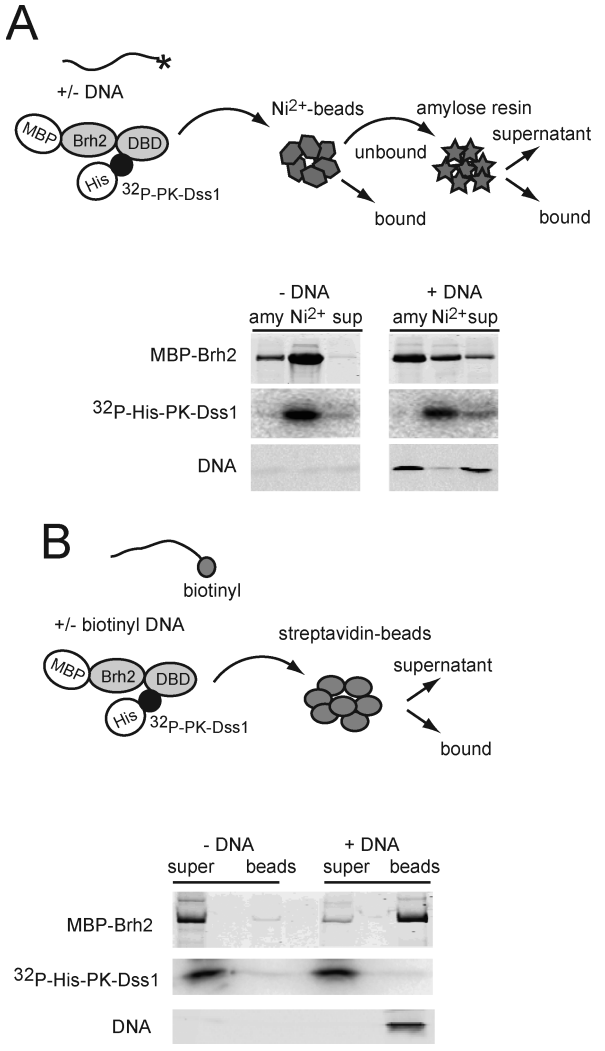

FIGURE 4: Dss1 is not associated with Brh2 bound to DNA. (A) MBP-Brh2 complexed with ^{32}P-labeled His-PK-Dss1 was added to reaction mixes with or without IRD800 ss60mer DNA. After 20 min, each mix was transferred to a tube containing Ni^{2+}-NTA beads (as a packed slurry) and held on ice for 10 min. After brief centrifugation, the beads were collected and the supernatant containing the unbound protein fraction was then transferred to a tube containing amylose beads. After 10 min, the beads were collected and the bound fractions from both Ni^{2+}-NTA (Ni^{2+}) and amylose (amy) with the final supernatant (sup) were analyzed for protein and DNA composition after SDS gel electrophoresis. Brh2 was visualized by protein staining, Dss1 by phosphorimaging, and DNA by fluorescence detection. (B) MBP-Brh2 complexed with ^{32}P-labeled His-PK-Dss1 was added to reaction mixes with or without 3′-biotin-labeled ss60mer DNA containing IRD700-labeled complementary strand as a tracer. After incubation for 40 min, mixes were transferred to a tube containing streptavidin-coated magnetic particles. After the beads had been collected, protein and DNA in the bound and supernatant fractions were analyzed by SDS gel electrophoresis.

decrease in the level of DNA binding (Figure 5A). These results suggest that the activity of Dss1 in inhibiting Brh2 from binding DNA is mediated through the C-terminal Dss1-interacting region and is not due simply to competition between Dss1 and DNA for a common binding site.

We asked whether there was specificity in the inhibition of DNA binding by Dss1 or whether the inhibition was due to an electrostatic effect based on the high acidic content of Dss1. To answer this, we took advantage of a Dss1 mutant protein altered by a change in a single aspartic acid residue to alanine ($Dss1^{D37A}$). The mutation causes a loss of DNA repair activity as determined by the failure to complement the radiation sensitivity of the *dss1* mutant upon expression of $Dss1^{D37A}$ (Figure 5B). Residue D37 corresponds to D16 of mammalian DSS1, which contacts K2671 in the mouse BRCA2 DBD (or K2750 in the human form). As the D37A mutation reduces the total ionic charge by only 5%, the mutant protein should still retain substantial activity in inhibiting the ability of Brh2 to bind DNA if the inhibition is due to a generalized electrostatic repulsion. On the other hand, if regulation of DNA binding by Dss1 is mediated through specific interactions at a functional interface as supported by the intermolecular aspartate−lysine contact in the atomic structure, the mutant should be unable to inhibit DNA binding by Brh2. Experimentally, we observed that

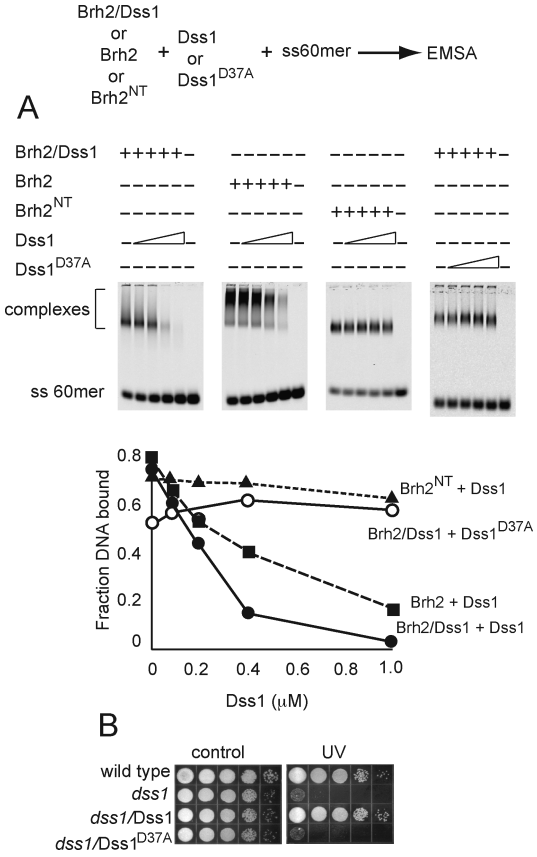

FIGURE 5: Dss1 attenuates the DNA binding activity of the Brh2−Dss1 complex. (A) To DNA binding reaction mixtures containing IRD800-labeled ss60mer (3.3 nM) and Brh2−His-Dss1, Brh2, or $Brh2^{NT}$ (100 nM) were added increasing levels of His-Dss1 or His-$Dss1^{D37A}$ to the lanes as indicated (0.1, 0.2, 0.4, and 1.0 μM, respectively). After incubation for 20 min, DNA binding was assessed. (B) Survival of the *dss1* deletion strain expressing Dss1 or $Dss1^{D37A}$ assessed after a UV dose of 120 J/m^2.

$Dss1^{D37A}$ did not inhibit Brh2's DNA binding activity, indicating that specificity for that particular residue is indeed important. Taken together, these observations suggest that the N-terminal DNA binding domain of Brh2 is modulated by allosteric control through the C-terminal region.

Dissociation of the Brh2−Dss1 Complex Facilitated by the Brh2 N-Terminal Region. If binding of DNA through the strong, primary interacting domain in the N-terminal region of Brh2 is negatively regulated by interaction of Dss1 with the C-terminal region, then it seems likely there must be signaling, likely a conformational change, transmitted between the two domains. Consistent with this notion, the $Brh2^{CT}$−Dss1 complex did not dissociate when incubated with DNA (Figure 6A,B), in contrast to dissociation of the Brh2−Dss1 complex promoted by DNA (Figure 3). Furthermore, when $Brh2^{NT}$ was added as a separate component to the $Brh2^{CT}$−Dss1 complex, there was no enhanced dissociation of the complex (Figure 6C). These observations reinforce the notion that DNA binding and Dss1 dissociation are counterbalanced through a mechanism involving structural change that propagates between the N-terminal and C-terminal regions of Brh2.

Brh2 Free of Dss1 Binds DNA Rapidly and Reassociates with Dss1. From the initial observations in this study that the strong binding of DNA upon addition of Brh2−Dss1 is correlated with dissociation of Dss1 and that excess Dss1 inhibits DNA binding, a two-ligand model is suggested. Namely, DNA

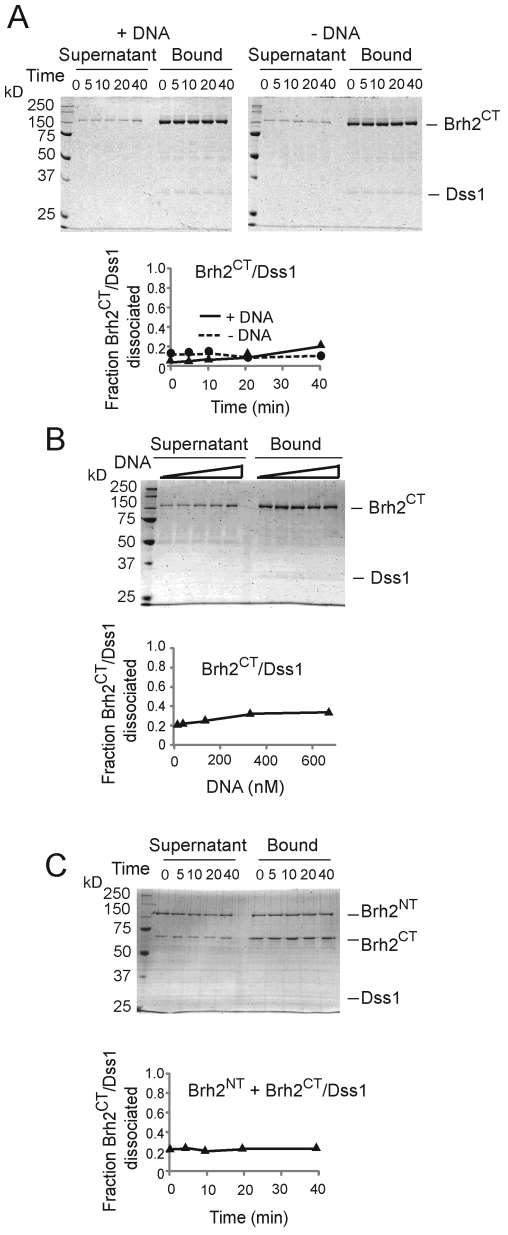

FIGURE 6: Brh2 N-terminal domain that is required for dissociation of Dss1. (A) The $Brh2^{CT}$−His-Dss1 complex (550 nM) was incubated at 37 °C in the presence or absence of DNA (130 nM unlabeled ss60mer). At the indicated times (minutes), Ni^{2+}-NTA beads were added to pull down His-Dss1 either free or complexed with $Brh2^{CT}$. The protein composition in the supernatant or bound fractions was determined by SDS gel electrophoresis. Protein was visualized by staining with SimplyBlue SafeStain (Invitrogen). The time course of dissociation is shown graphically. (B) Reaction mixes contained the $Brh2^{CT}$−His-Dss1 complex (550 nM), and increasing concentrations of DNA (20, 40, 130, 330, and 660 nM from left to right) were incubated for 20 min. (C) The reaction mix contained the $Brh2^{CT}$−His-Dss1 complex (550 nM) and $Brh2^{NT}$(550 nM). In this case, $Brh2^{NT}$ was tagged with MBP and His whereas the MBP tag was removed from $Brh2^{CT}$ by cleavage with TEV protease. At the indicated times, Ni^{2+}-NTA beads were added to pull down His-Dss1 and the protein composition in the supernatant and bound fractions was determined.

and Dss1 negatively regulate each other's association with Brh2. Corroborating support for this model should be able to be obtained via simple mass action experiments. Two predictions should be satisfied. First, Brh2 stripped of Dss1 should bind DNA quickly, and second, Dss1 should be capable of associating

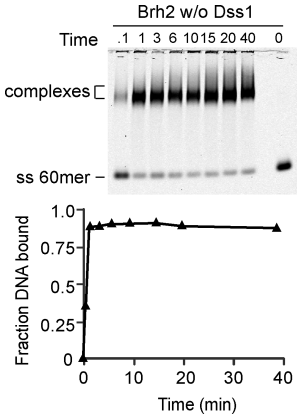

FIGURE 7: DNA binding rate of the Brh2 apoprotein. The time course of DNA binding was determined with IRD800-labeled ss60mer (3.3 nM) and 100 nM Brh2 stripped of Dss1 prepared as described in Experimental Procedures. Aliquots were removed from binding reaction mixtures at the indicated times (minutes) and fixed with glutaraldehyde, and the DNA was analyzed for mobility shift after electrophoresis. For the zero time point, DNA was added to a Brh2 reaction mixture already containing glutaraldehyde.

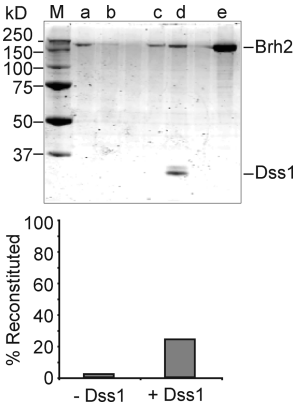

FIGURE 8: Reconstitution of the Brh2−Dss1 complex. Reaction mixtures containing the Brh2 apoprotein were mixed with His-Dss1. After 1 h at 4 °C, Ni^{2+}-NTA beads were added, washed, and then eluted with SDS sample buffer (80 μL). Aliquots (10 μL) of the supernatant (first wash) and bound fractions were separated by SDS gel electrophoresis. After being stained with SimplyBlue SafeStain, bands were quantitated using the Odyssey detection platform: lane a, supernatant, without Dss1; lane b, bound, without Dss1; lane c, supernatant, with Dss1; lane d, bound, with Dss1; lane e, 12.5% of total Brh2 apoprotein initially added to the reaction; lane M, size standards.

with Brh2 in the absence of DNA. Unfortunately, obtaining Brh2 free of Dss1 has been problematic because Brh2 expressed in *E. coli* in the absence of Dss1 is prone to aggregation and is highly susceptible to proteolytic degradation. Brh2 coexpressed with Dss1, however, is not subject to those problems and exhibits hydrodynamic properties consistent with behavior of a monomeric protein during gel filtration (*8*, *11*). Therefore, we used the Brh2−Dss1 complex as starting material and devised a procedure for preparing Brh2 free of Dss1. The approach we took was the empirical one of searching for a condition favoring dissociation of the Brh2−Dss1 complex. Then we took advantage of the affinity tags on Brh2 and Dss1 to isolate the Brh2 apoprotein directly or else deplete the preparation of Dss1. Of many conditions tested, the promising one was that in which divalent cations were effective in promoting dissociation of the Brh2−Dss1 complex. We determined that holding the complex in a buffer with 20 mM Mg^{2+} resulted in dissociation of Brh2 from Dss1. By incorporating a Mg^{2+} incubation step in the purification procedure, coupled with affinity purification, we were able to isolate the Brh2 protein largely free of Dss1. Nevertheless, the protein in this form was difficult with which to work, as it was highly sensitive to the slightest trace of protease contamination and also appeared to be prone to aggregation. We have encountered variability in experiments using Brh2 apoprotein and attribute this to its unstable nature.

We monitored DNA binding by the Brh2 apoprotein and indeed observed that the time course exhibited no delay and appeared to be comparable to that of $Brh2^{NT}$ in the rapid rate of association (Figure 7). The DNA binding activity of the Brh2 apoprotein was also inhibited by addition of Dss1 (Figure 5). We tested for reassociation of His-Dss1 with Brh2 apoprotein using the pull-down procedure with Ni^{2+}-NTA beads to capture His-tagged Dss1. After Brh2 was incubated in a reaction mix containing an 8-fold molar excess of His-Dss1, a substantial fraction of the Brh2 became capable of associating with the Ni^{2+}-NTA resin in a Dss1-dependent manner (Figure 8). Using this procedure, we estimated that ~70% of the Brh2 initially added to the reaction tube could be identified after recovery in the bound and supernatant fractions. Of this total recovered amount, we estimate that 24% had reassociated with His-Dss1 (Figure 8B). A minor fraction of Brh2 (1.3%) was found associated with the Ni^{2+}-NTA beads in the absence of His-Dss1. Thus, the Brh2 present in the bound fraction is due to specific interaction with His-Dss1. We do not know as yet the factors or conditions that would favor more extensive reassociation of Dss1, but with variation of salt, temperature, divalent cation, etc., it seems likely that the reverse reaction could be optimized empirically. In summary, these observations suggest that an equilibrium between Dss1-bound and Dss1-free forms of Brh2 is important in DNA binding and support the idea that accessibility of Brh2 to DNA is governed by Dss1.

DISCUSSION

There are two principal conclusions from this study. First, the DNA binding potential of Brh2 is linked to a change in the state of the protein that is mediated by Dss1. Second, DNA and Dss1 serve as counterbalancing ligands that attenuate each other's association with Brh2. These findings suggest that Brh2 function involves dynamic conformational changes in domain configuration that are regulated by Dss1, in essence allostery.

We have established that Dss1 is crucial for proficiency in DNA repair and recombination in *U. maydis* and made the argument that it serves to regulate Brh2 function (*12*, *15*). That Dss1 serves as a regulator is supported by the observation that variant forms of Brh2 with the Dss1-interacting region deleted, indeed the entire canonical Dss1−DNA binding domain, are liberated from an inactive state and exhibit resistance to radiation, enable formation of subnuclear Rad51 foci in cells following DNA damage, and are recombination proficient (*15*). The N-terminal region of Brh2 has a strong DNA binding domain with properties that apparently make possible all the DNA-interactive operations attributable to the full-length protein (*16*). With the added Rad51-interacting BRC element, it would seem that the N-terminal region of Brh2 constitutes a module endowed with all of the abilities to engage Rad51 and to deliver it to DNA (*15*). The positive and direct role of the N-terminal region of Brh2 in Rad51 presentation appears to be balanced by forces imposed from the C-terminal region. This is most apparent in

studies on recombination in which the frequency of gap repair as well as the rate of spontaneous allelic recombination is higher in cells expressing $Brh2^{NT}$ as compared to the full-length protein (*15*). Additional support comes from studies with a mutant defective in the RecQ helicase Blm. Toxic recombination-dependent DNA structures formed during replication stress in the presence of hydroxyurea are not generated in *blm brh2* double mutant cells expressing $Brh2^{NT}$ in contrast to the full-length protein (*22*). In previous work, it was found that a second Rad51-interacting element, CRE, unrelated to BRC was present at the extreme C-terminus of Brh2 (*11*). These elements appear to work together in some way to impose appropriate and controlled recombinational activity, and Dss1 appears to mediate their communication. This finding showing that Dss1 governs interaction of DNA with the primary binding site within the N-terminus of Brh2 adds another layer of knowledge and some additional insight into the mechanism.

We imagine two different models that could account for the observations. In one view, Dss1 occludes DNA from binding to the primary N-terminal DNA binding domain by imposing an unfavorable conformation mediated through the C-terminal region. Here the Dss1-bound form of Brh2 is imagined in equilibrium with the unbound form, although the equilibrium lies far to the left (bound form). Upon dissociation of Dss1, the conformation changes and the N-terminal DNA binding site becomes available for association with DNA. Since Dss1 does not appear to associate with $Brh2^{NT}$ or compete with it for binding DNA, Brh2 is likely in a conformational state when Dss1 is bound that prevents binding of DNA to the N-terminal DNA binding domain. A change resulting from Dss1 dissociation enables DNA binding. An alternative model is that in which DNA binds to the dominant N-terminal DNA binding domain and through an induced fit a conformational change that causes ejection of Dss1 ensues.

In favor of the latter mechanism (DNA binds first) is the finding that with increasing concentrations of DNA added to Brh2−Dss1 complexes, the greater the fraction of Brh2 that dissociates from Dss1. In support of the former mechanism (Dss1 dissociates first) is the finding that binding of DNA to Brh2−Dss1 appears to be slow compared to binding to $Brh2^{NT}$, implying that another step is rate-limiting in the DNA binding reaction. We imagine this step is a conformational change concomitant with the dissociation of Dss1. There are no doubt other possibilities, and of course, these views might be oversimplified. Perhaps it is naïve to view DNA and Dss1 as model ligands that are mutually exclusive. Their associations with Brh2 may not be accurately represented in terms of a simple "on" or "off" state when there could be multiple attachment points. In the case of Dss1, in which there could be multidentate association with Brh2, maybe the transient loosening of one site is enough to open contacts for association with DNA without the physical separation of Dss1. For instance, it could also be argued that the observed time delay in DNA binding is consistent with the induced fit model in which DNA binds first to force out Dss1. In this case, one would have to stipulate that the initial DNA binding is weak so that the protein−DNA encounter complexes formed are not strong enough to be immediately detected by our methods. Then as Dss1 is ejected there would follow the formation of a DNA-bound complex that would become stronger over time as more and more contacts were formed between surfaces. Further experimentation will be required to distinguish between the models.

In summary, it appears that the activation of Brh2 for DNA binding coincides with the dissociation of Dss1. Concomitant with this is conversion of Brh2 to a dimeric or even higher-order form (*11*). The mechanism, however, by which delivery of Rad51 to sites of DNA damage is coupled to these structural changes in Brh2 is not understood. It seems evident that interplay between Dss1 and the cognate interaction site within the C-terminal region of Brh2 provides a means for fine-tuning recombination. In the absence of this entire region, Rad51 foci persist longer and allelic recombination and gap repair occur at significantly higher frequencies than in wild-type cells (*15*). Given the well-documented relationship between genomic instability and an elevated level of recombination, it can be imagined that such an increase might well be detrimental. We have no information at present about how the DNA binding domain represented by the C-terminal OB folds contributes to attenuating recombination or how the C-terminal Rad51-interacting element CRE takes part. However, it seems likely that Rad51 filament quality is compromised somehow because cells expressing only $Brh2^{NT}$ are more sensitive to high doses of UV (*15*). This is especially apparent in cells also lacking the Rad51 paralog Rec2 (*10*, *16*).

Finally, there is the broader question of why interaction of Brh2 with DNA is regulated by Dss1. In other words, what biological purpose is served by coupling the dependence of Brh2 activity with its state of association with Dss1? Bioinformatics analysis with disorder prediction programs such as IUPred (*23*) or FoldIndex (*24*) indicates Dss1 to be predominately lacking in secondary structure (data not shown), but as one can clearly see from the crystal structure of the mammalian BRCA2 DBD, regions of Dss1 fold into an ordered state when associated with this interacting partner and concomitantly impose stability on the partner (*13*). Thus, Dss1 might be considered as a type of chaperone, but on the basis of the observations described above, it would appear that Dss1 is appropriately and more generally categorized as an intrinsically unstructured or disordered protein, an emerging class of proteins recognized for mediating signaling and regulation of many biological systems (*25*−*27*). Besides its role in DNA repair and recombination, Dss1 has been shown to function in mRNA processing (*28*−*30*)and to serve as an integral component of the 19S regulatory subunit of the proteasome (*31*−*33*). Thus, Dss1 appears to function as a hub linking several diverse cellular networks. Understanding the details of the interaction of Dss1 with Brh2 will be important for understanding why a crucial DNA repair pathway is dependent on such a regulatory mechanism and could lead to insight into a more general understanding of how DNA repair is coupled to the major cellular systems of RNA and protein processing.

ACKNOWLEDGMENT

We thank Dr. Lorraine Symington (Columbia University, New York, NY) for critical comments on the science and manuscript.

REFERENCES

1. San Filippo, J., Sung, P., and Klein, H. (2008) Mechanism of eukaryotic homologous recombination. *Annu. Rev. Biochem. 77*, 229–257.
2. Pellegrini, L., and Venkitaraman, A. (2004) Emerging functions of BRCA2 in DNA recombination. *Trends Biochem. Sci. 29*, 310–316.
3. Thorslund, T., and West, S. C. (2007) BRCA2: aA universal recombinase regulator. *Oncogene 26*, 7720–7730.
4. Davies, A. A., Masson, J. Y., McIlwraith, M. J., Stasiak, A. Z., Stasiak, A., Venkitaraman, A. R., and West, S. C. (2001) Role of

BRCA2 in control of the RAD51 recombination and DNA repair protein. *Mol. Cell 7*, 273–282.
5. Davies, O. R., and Pellegrini, L. (2007) Interaction with the BRCA2 C terminus protects RAD51-DNA filaments from disassembly by BRC repeats. *Nat. Struct. Mol. Biol. 14*, 475–483.
6. Esashi, F., Galkin, V. E., Yu, X., Egelman, E. H., and West, S. C. (2007) Stabilization of RAD51 nucleoprotein filaments by the C-terminal region of BRCA2. *Nat. Struct. Mol. Biol. 14*, 468–474.
7. Galkin, V. E., Esashi, F., Yu, X., Yang, S., West, S. C., and Egelman, E. H. (2005) BRCA2 BRC motifs bind RAD51-DNA filaments. *Proc. Natl. Acad. Sci. U.S.A. 102*, 8537–8542.
8. Yang, H., Li, Q., Fan, J., Holloman, W. K., and Pavletich, N. P. (2005) The BRCA2 homologue Brh2 nucleates RAD51 filament formation at a dsDNA-ssDNA junction. *Nature 433*, 653–657.
9. Mazloum, N., and Holloman, W. K. (2009) Second-end capture in DNA double-strand break repair promoted by Brh2 protein of *Ustilago maydis*. *Mol. Cell 33*, 160–170.
10. Kojic, M., Zhou, Q., Lisby, M., and Holloman, W. K. (2006) Rec2 interplay with both Brh2 and Rad51 balances recombinational repair in *Ustilago maydis*. *Mol. Cell. Biol. 26*, 678–688.
11. Zhou, Q., Kojic, M., Cao, Z., Lisby, M., Mazloum, N. A., and Holloman, W. K. (2007) Dss1 interaction with Brh2 as a regulatory mechanism for recombinational repair. *Mol. Cell. Biol. 27*, 2512–2526.
12. Kojic, M., Yang, H., Kostrub, C. F., Pavletich, N. P., and Holloman, W. K. (2003) The BRCA2-interacting protein DSS1 is vital for DNA repair, recombination, and genome stability in *Ustilago maydis*. *Mol. Cell 12*, 1043–1049.
13. Yang, H., Jeffrey, P. D., Miller, J., Kinnucan, E., Sun, Y., Thoma, N. H., Zheng, N., Chen, P. L., Lee, W. H., and Pavletich, N. P. (2002) BRCA2 function in DNA binding and recombination from a BRCA2-DSS1-ssDNA structure. *Science 297*, 1837–1848.
14. Kojic, M., Kostrub, C. F., Buchman, A. R., and Holloman, W. K. (2002) BRCA2 homolog required for proficiency in DNA repair, recombination, and genome stability in *Ustilago maydis*. *Mol. Cell 10*, 683–691.
15. Kojic, M., Zhou, Q., Lisby, M., and Holloman, W. K. (2005) Brh2-Dss1 interplay enables properly controlled recombination in *Ustilago maydis*. *Mol. Cell. Biol. 25*, 2547–2557.
16. Zhou, Q., Kojic, M., and Holloman, W. K. (2009) DNA-binding domain within Brh2 N-terminus is the primary interaction site for association with DNA. *J. Biol. Chem. 284*, 8265–8273.
17. Kojic, M., Mao, N., Zhou, Q., Lisby, M., and Holloman, W. K. (2008) Compensatory role for Rad52 during recombinational repair in *Ustilago maydis*. *Mol. Microbiol. 67*, 1156–1168.
18. Ho, S. N., Hunt, H. D., Horton, R. M., Pullen, J. K., and Pease, L. R. (1989) Site-directed mutagenesis by overlap extension using the polymerase chain reaction. *Gene 77*, 51–59.
19. Mazloum, N., Zhou, Q., and Holloman, W. K. (2007) DNA binding, annealing, and strand exchange activities of Brh2 protein from *Ustilago maydis*. *Biochemistry 46*, 7163–7173.
20. Wong, I., and Lohman, T. M. (1993) A double-filter method for nitrocellulose-filter binding: Application to protein-nucleic acid interactions. *Proc. Natl. Acad. Sci. U.S.A. 90*, 5428–5432.
21. Fancy, D. A., Melcher, K., Johnston, S. A., and Kodadek, T. (1996) New chemistry for the study of multiprotein complexes: The six-histidine tag as a receptor for a protein crosslinking reagent. *Chem. Biol. 3*, 551–559.
22. Mao, N., Kojic, M., and Holloman, W. K. (2009) Role of Blm and collaborating factors in recombination and survival following replication stress in *Ustilago maydis*. *DNA Repair 8*, 752–759.
23. Dosztanyi, Z., Csizmok, V., Tompa, P., and Simon, I. (2005) IUPred: Web server for the prediction of intrinsically unstructured regions of proteins based on estimated energy content. *Bioinformatics 21*, 3433–3434.
24. Prilusky, J., Felder, C. E., Zeev-Ben-Mordehai, T., Rydberg, E. H., Man, O., Beckmann, J. S., Silman, I., and Sussman, J. L. (2005) FoldIndex: A simple tool to predict whether a given protein sequence is intrinsically unfolded. *Bioinformatics 21*, 3435–3438.
25. Dyson, H. J., and Wright, P. E. (2005) Intrinsically unstructured proteins and their functions. *Nat. Rev. Mol. Cell Biol. 6*, 197–208.
26. Galea, C. A., Wang, Y., Sivakolundu, S. G., and Kriwacki, R. W. (2008) Regulation of cell division by intrinsically unstructured proteins: Intrinsic flexibility, modularity, and signaling conduits. *Biochemistry 47*, 7598–7609.
27. Wright, P. E., and Dyson, H. J. (2009) Linking folding and binding. *Curr. Opin. Struct. Biol. 19*, 31–38.
28. Thakurta, A. G., Gopal, G., Yoon, J. H., Kozak, L., and Dhar, R. (2005) Homolog of BRCA2-interacting Dss1p and Uap56p link Mlo3p and Rae1p for mRNA export in fission yeast. *EMBO J. 24*, 2512–2523.
29. Wilmes, G. M., Bergkessel, M., Bandyopadhyay, S., Shales, M., Braberg, H., Cagney, G., Collins, S. R., Whitworth, G. B., Kress, T. L., Weissman, J. S., Ideker, T., Guthrie, C., and Krogan, N. J. (2008) A genetic interaction map of RNA-processing factors reveals links between Sem1/Dss1-containing complexes and mRNA export and splicing. *Mol. Cell 32*, 735–746.
30. Faza, M. B., Kemmler, S., Jimeno, S., Gonzalez-aguilera, C., Aguilera, A., Hurt, E., and Panse, V. G. (2009) Sem1 is a functional component of the nuclear pore complex-associated messenger RNA export machinery. *J. Cell Biol. 184*, 833–846.
31. Funakoshi, M., Li, X., Velichutina, I., Hochstrasser, M., and Kobayashi, H. (2004) Sem1, the yeast ortholog of a human BRCA2-binding protein, is a component of the proteasome regulatory particle that enhances proteasome stability. *J. Cell Sci. 117*, 6447–6454.
32. Krogan, N. J., Lam, M. H., Fillingham, J., Keogh, M. C., Gebbia, M., Li, J., Datta, N., Cagney, G., Buratowski, S., Emili, A., and Greenblatt, J. F. (2004) Proteasome involvement in the repair of DNA double-strand breaks. *Mol. Cell 16*, 1027–1034.
33. Sone, T., Saeki, Y., Toh-e, A., and Yokosawa, H. (2004) Sem1p is a novel subunit of the 26 S proteasome from *Saccharomyces cerevisiae*. *J. Biol. Chem. 279*, 28807–28816.